Supplement of Atmos. Chem. Phys., 14, 9677–9694, 2014
http://www.atmos-chem-phys.net/14/9677/2014/
doi:10.5194/acp-14-9677-2014-supplement

Atmospheric Chemistry and Physics Open Access

Supplement of

Links between satellite-retrieved aerosol and precipitation

E. Gryspeerdt et al.

Correspondence to: E. Gryspeerdt (gryspeerdt@atm.ox.ac.uk)

Supplementary Information

E. Gryspeerdt, P. Stier and D. G. Partridge

A Reflectivity profiles

Estimates of precipitation rates based on microwave emission are known to suffer from retrieval errors over land, with assumptions about surface emissivity not always being valid (Wilheit, 1986; Greenwald et al., 2007). Microwave instruments are also known to have issues separating cloud water from rain water, such that a change in cloud water may appear as a precipitation change (Berg et al., 2006). Whilst active microwave instruments such as the TRMM PR also suffer from errors in their retrievals, they do not have the same difficulties distinguishing between cloud and rainwater. Both active (such as the TRMM PR) and passive microwave retrievals make assumptions about droplet size. Here we investigate changes in the TRMM PR reflectivity, which includes comparatively few assumptions. Precipitation estimates from the TRMM PR are included in the TRMM 3B42 product. However, as the majority of the 3B42 product is determined using passive microwave and IR instruments, the radar reflectivity presents a semi-independent evaluation of precipitation properties.

The TRMM PR cannot detect very light rain, having a minimum detectable signal of about 15 dbZ (Nesbitt et al., 2000). Although it is not able to capture the entire spectrum of rainfall events, it is not sensitive to cloud water, so changes in the PR reflectivity are due to changes in rainfall properties, rather than cloud properties.

We use the TRMM PR reflectivity profiles from the TRMM 2A25 radar reflectivity product to investigate the development of radar reflectivity within the cloud regimes and how it changes as a function of retrieved AI, in the same way as with the 3B42 precipitation product. We investigate the frequency of occurrence of reflectivity retrievals above 20 dbZ as a proxy for raining pixels. An increase in the occurrence of retrievals above 20 dbZ suggests an increase in precipitation occurrence (eg. Liu and Zipser, 2008).

The diurnal cycle of reflectivity (Fig. A.1) shows many similar features to the diurnal cycle of precipitation (Fig. 2). Over ocean, only the thick mid-level (Fig. A.1b) and the deep convective regimes (Fig. A.1f) show a maximum in 20 dbZ occurrence at T+0, with all of the other regimes showing a minimum. This is due to the low frequency of occurrence and weak diurnal cycle over ocean generating an artificial peak in the reflectivity at T+0 for these regimes, a peak also seen in the 3B42 precipitation rate (Fig. 2m). Over land (Fig. A.1h-n), there is a peak in the reflectivity after T+0 for all of the regimes. For each of the regimes over land, the frequency of occurrence of 20 dbZ reflectivities is higher than over ocean.

In the regimes dominated by heavy precipitation (Thick mid level and deep convective) we find results supporting those found using the 3B42 product (Fig. A.2i,m). The thick mid-level regime (Fig. A.2i) and the deep convective regimes over land (Fig. A.2m) show an increase in high reflectivities in the high AI population at times after T+0, whilst also showing a decrease in reflectivities at times before T+0, which we have suggested is due to wet scavenging. Over ocean, the results, especially for the deep convective regime, are noisier and so harder to interpret. Many of the other regimes, especially over land, show lower reflectivities in the high AI population at times before the AI retrieval, consistent with wet scavenging removing more aerosol at higher rainrates.

The stratocumulus (Fig. A.2n) and transition (Fig. A.2k) regimes over land do not show a large increase in reflectivity at times after T+0, although there is a small increase in reflectivity in both of these regimes, which is significant at higher altitudes. In the shallow cumulus regime over land, there is a small decrease in the occurrence of reflectivities above 20 dbZ, in apparent contrast to the 3B42 precipitation retrievals, which show an increase in precipitation

(which would usually be associated with an increase in reflectivity). It is possible that this lack of reflectivity increase with increasing AI when observed by the radar is due to an increase in very light precipitation, which might be detected by the microwave instruments and not the radar (Kummerow et al., 1998). It is also possible that the increase in precipitation detected by the 3B42 product is due to an increase in cloud water, or some other change in cloud properties, rather than a change in precipitation, although the increase in Lightning Imaging Sensor (LIS) flash rate (Fig. 9) suggests there is still an invigoration. Passive microwave instruments can have difficulties determining precipitation over land (Bauer et al., 2005), and although the high frequency channels typically used over land are less susceptible to influences from surface properties, the link to precipitation properties is not as direct as with the low frequency channels (Stephens et al., 2008). The extra assumptions made when determining precipitation over land might explain the differences in the effects of aerosols on retrieved precipitation and radar reflectivity.

Although the TRMM PR is not able to retrieve very light precipitation, we can use it to investigate the regional dependence of the T+0→+6 mean precipitation rate for the shallow cumulus regime (Fig. 4a). For each of the four regions highlighted (in Fig. 4a), we create a reflectivity–height histogram (Fig. A.3a,e,i,m) (eg. L'Ecuyer et al., 2009). These histograms are very similar for each of the regions, suggesting that there is not a fundamental property of the precipitation in the shallow cumulus regime that is different between these regions. The difference in the histograms between the high and low AI populations over the T+0→+6 period (Fig. A.3b,f,j,n) shows effects supporting the results found when using the 3B42 precipitation product.

The Central Pacific and Seychelles regions show an increase in high reflectivities over the T+0→+6 period and a corresponding reduction in the number of pixels with less than 12 dbZ reflectivities in the high AI population (leftmost column in Figs. A.3f,j). This suggests that there is an increase in precipitation at high AI after T+0 in these regions, rather than just a modification of the cloud properties. These changes in reflectivity are consistent with the precipitation changes observed in the 3B42 product (Fig. 4a). When considering only the pixels with reflectivities above 12 dbZ in these regions (Fig. A.3h), we see a shift to higher reflectivities, suggesting that the distribution of precipitation has changed. This indicates not only an increase in the frequency of occurrence of precipitation events, but an increase in the intensity of these events.

The Arabian Sea region shows a decrease in reflectivities with increasing AI over the T+0→+6 period (Fig. A.3b), suggesting a decrease in precipitation with increasing AI. This reflects the precipitation change seen in the 3B42 product, where we also see a decrease in precipitation with increasing AI over the T+0→+6 period (Fig. 4a). Similar effects are observed in the China Sea region (Fig. A.3n), with a decrease in the occurrence of reflectivities above 12 dbZ in the high AI population compared to the low AI population over this period. The decrease in occurrence in reflectivities above 12 dbZ in the period T-9→-3 for the high AI population (Fig. A.3o) is sensitive to large scale RH in this region, even after accounting for CF variations with AI (not shown). The sensitivity to large scale RH is likely due to related variations in column water vapour, which is well correlated to differences between passive microwave and radar precipitation retrievals (Berg et al., 2006).

B Development of meteorological properties

Although we account for the influence of meteorological properties at the time of the AI retrieval (T+0), reanalysis products are known to not be a perfect representation of the atmosphere (eg. Wang et al., 2011). There is a possibility that the aerosol retrieval is more sensitive to certain meteorological conditions than the reanalysis dataset. If we see a divergence in the reanalysis meteorology between the high and low AI populations after T+0 this would suggest that the re-analysis data is not as sensitive to the meteorological parameters as we need it to be.

We investigate the 500 hPa vertical velocity (ω_{500}), as it is strongly related to precipitation, especially in convective clouds (Koren et al., 2010; Medeiros and Stevens, 2011). We find a strong link between AI and ω_{500} (Fig. B.1a,b), especially over ocean. The effect is similar to the observed relationship between AI and precipitation, with lower values of ω_{500} (rising air) correlated to higher precipitation rates. We find the expected link between precipitation and ω_{500}, with the more heavily precipitating regimes having a lower mean ω_{500} at T+0. The strong link between AI and ω_{500}, coupled with the ω_{500}-precipitation correlation could allow ω_{500} to act as a controlling variable in the AI-precipitation correlation, in the same way as CF does (Gryspeerdt et al., 2014). This further emphasises the importance of accounting for the initial cloud fraction and meteorological state.

The majority of regimes show very little difference

in the ω_{500} development between the low and high AI populations, once the variance in ω_{500} at T+0 is accounted for (Fig. B.1). Where a difference is observed, such as for the shallow cumulus (Fig. B.1d) regime over land, this appears to be due to small errors in the accounting for the variation at T+0, rather than a difference in the environment of the regimes, and so is unlikely to be producing our observed results. This suggests that we have adequately accounted for the correlation between AI at meteorological properties at T+0.

C Additional satellite products

As the 3B42 retrieval includes some IR precipitation data, we repeat our analysis using the 3B42 'HQ' product, which includes only the non-gauge adjusted microwave data (Fig. C.1).

We also repeat our analysis excluding points where the retrieved precipitation is zero (Fig. C.2). This analysis is not included in the main analysis, as it removes the ability to study the complete lifecycle of clouds. We see increases in precipitation after T+0 for the high AI population compared to the low AI population, similar to those seen when using the complete 3B42 product. This suggests that the increase in precipitation occurs from an intensification of precipitation in already-precipitating clouds, rather than a change in precipitation initiation (although that is still likely to be important).

The precipitation development analysis repeated using GlobAerosol AATSR daily AOD data (Fig. C.3). As AATSR is flown on the Envisat satellite, T+0 is shifted to 1000 LST, making Fig. 3 the most suitable comparison. The plots using AATSR AOD are noisier than those using MODIS data, due to a smaller swath reducing the available data. Only the all data and the shallow cumulus regime precipitation development plots are shown.

To demonstrate that the observed increase in precipitation observed at times after T+0 for the high AI population is not a consequence of a reduced precipitation rate at times before T+0 in the high AI population, we also show the precipitation development of each regime where the regimes are separated by the precipitation rate at T-3 (Fig. C.4). The red line shows the precipitation development within each regime of the quartile with the highest precipitation rate and the blue line in the lower precipitation rate quartile at T-3. It is clear that a low precipitation rate at times T-3 is not correlated with a high precipitation rate at times after T+0. The CF distributions for the high and low precipitation rate quartiles have been sampled so that they are the same at T+0.

D Surface precipitation

To compare our results against a 'ground-truth' precipitation product, we also use precipitation retrievals from the UK Met. Office MIDAS database (UK Meteorological Office, 2012). This includes precipitation data from multiple rain-gauges at a time resolution of three hours or lower. We are restricted in the total number of sites by the need to use sub-daily temporal resolution, which is not commonly supplied in gauge datasets.

Both the TRMM PR and the merged product require assumptions about the droplet size distribution to determine the precipitation rate, especially over land (Iguchi and Meneghini, 1994; Stephens et al., 2008). As one possible effect of aerosols is to modify the droplet size distribution, we cannot be certain an increase in retrieved precipitation is due to a increased precipitation rate. A shift in the droplet size distribution towards larger droplets without an increase in the total precipitation amount could be interpreted by both active and passive microwave instruments as an increase in precipitation.

The only way to sure of an increase in precipitation is to use a surface measurement of precipitation. Unfortunately surface rain gauges are limited in their sampling compared to satellite instruments.

We make use of the UK Met Office MIDAS database of surface station data. This includes surface data from the study region, with precipitation data from a subset of stations at a temporal resolution of 3 or 6 hours. We average our data over three hour periods, rather than the single hour periods used for the merged precipitation product. Unfortunately, there is not enough rain gauge data available to make a determination about whether the satellite studies are seeing a change in surface precipitation. Although there are hints of effects, they are not significant.

The main issue appears to be the shortage of data for the rain gauges, ideally there would be a greater number of rain gauges than satellite datapoints so that the gauge data might be closer to the areal mean precipitation rate. The lack of sampling (Fig. D.1a) in regions with a particularly strong response in the satellite data (Fig. 4) is unfortunate.

References

Bauer, P., Moreau, E., and di Michele, S.: Hydrometeor Retrieval Accuracy Using Microwave

Window and Sounding Channel Observations., J. App. Met., 44, 1016–1032, doi:10.1175/JAM2257.1, 2005.

Berg, W., L'Ecuyer, T., and Kummerow, C.: Rainfall Climate Regimes: The Relationship of Regional TRMM Rainfall Biases to the Environment, J. App. Met. Clim., 45, 434–454, doi:10.1175/JAM2331.1, 2006.

Greenwald, T. J., L'Ecuyer, T. S., and Christopher, S. A.: Evaluating specific error characteristics of microwave-derived cloud liquid water products, Geophys. Res. Lett., 34, L22 807, doi:10.1029/2007GL031180, 2007.

Gryspeerdt, E., Stier, P., and Grandey, B.: Cloud fraction mediates the aerosol optical depth - cloud top height relationship, Geophys. Rev. Lett., 41, doi:10.1002/2014GL059524, 2014.

Iguchi, T. and Meneghini, R.: Intercomparison of Single-Frequency Methods for Retrieving a Vertical Rain Profile from Airborne or Spaceborne Radar Data, J. Atmos. Ocean Tech., 11, 1507–1516, doi:10.1175/1520-0426(1994)011⟨1507:IOSFMF⟩2.0.CO;2, 1994.

Koren, I., Feingold, G., and Remer, L.: The invigoration of deep convective clouds over the Atlantic: aerosol effect, meteorology or retrieval artifact?, Atmos. Chem. Phys., 10, 8855–8872, doi:10.5194/acp-10-8855-2010, 2010.

Kummerow, C., Barnes, W., Kozu, T., Shiue, J., and Simpson, J.: The Tropical Rainfall Measuring Mission (TRMM) Sensor Package, J. Atmos. Ocean Tech., 15, 809–817, doi:10.1175/1520-0426(1998)015⟨0809:TTRMMT⟩2.0.CO;2, 1998.

L'Ecuyer, T., Berg, W., Haynes, J., Lebsock, M., and Takemura, T.: Global observations of aerosol impacts on precipitation occurrence in warm maritime clouds, J. Geophys. Res., 114, D09 211, doi:10.1029/2008JD011273, 2009.

Liu, C. and Zipser, E. J.: Diurnal cycles of precipitation, clouds, and lightning in the tropics from 9 years of TRMM observations, Geophys. Res. Lett., 35, L04 819, doi:10.1029/2007GL032437, 2008.

Medeiros, B. and Stevens, B.: Revealing differences in GCM representations of low clouds, Climate Dyn., 36, 385–399, doi:10.1007/s00382-009-0694-5, 2011.

Nesbitt, S. W., Zipser, E. J., and Cecil, D. J.: A Census of Precipitation Features in the Tropics Using TRMM: Radar, Ice Scattering, and Lightning Observations., J. Climate, 13, 4087–4106, doi:10.1175/1520-0442(2000)013⟨4087:ACOPFI⟩2.0.CO;2, 2000.

Stephens, G., Vane, D., Tanelli, S., Im, E., Durden, S., Rokey, M., Reinke, D., Partain, P., Mace, G., Austin, R., L'Ecuyer, T., Haynes, J., Lebsock, M., Suzuki, K., Waliser, D., Wu, D., Kay, J., Gettelman, A., Wang, Z., and Marchand, R.: CloudSat mission: Performance and early science after the first year of operation, J. Geophys. Res., 113, D00A18, doi:10.1029/2008JD009982, 2008.

UK Meteorological Office: Met Office Integrated Data Archive System (MIDAS) Land and Marine Surface Stations Network (1853-current), URL `http://badc.nerc.ac.uk/view/badc.nerc.ac.uk__ATOM__dataent_ukmo-midas`, 2012.

Wang, W., Xie, P., Yoo, S.-H., Xue, Y., Kumar, A., and Wu, X.: An assessment of the surface climate in the NCEP climate forecast system reanalysis, Climate Dyn., 37, 1601–1620, doi:10.1007/s00382-010-0935-7, 2011.

Wilheit, T. T.: Some Comments on Passive Microwave Measurement of Rain., Bull. A. Met. Soc., 67, 1226–1232, doi:10.1175/1520-0477(1986)067⟨1226:SCOPMM⟩2.0.CO;2, 1986.

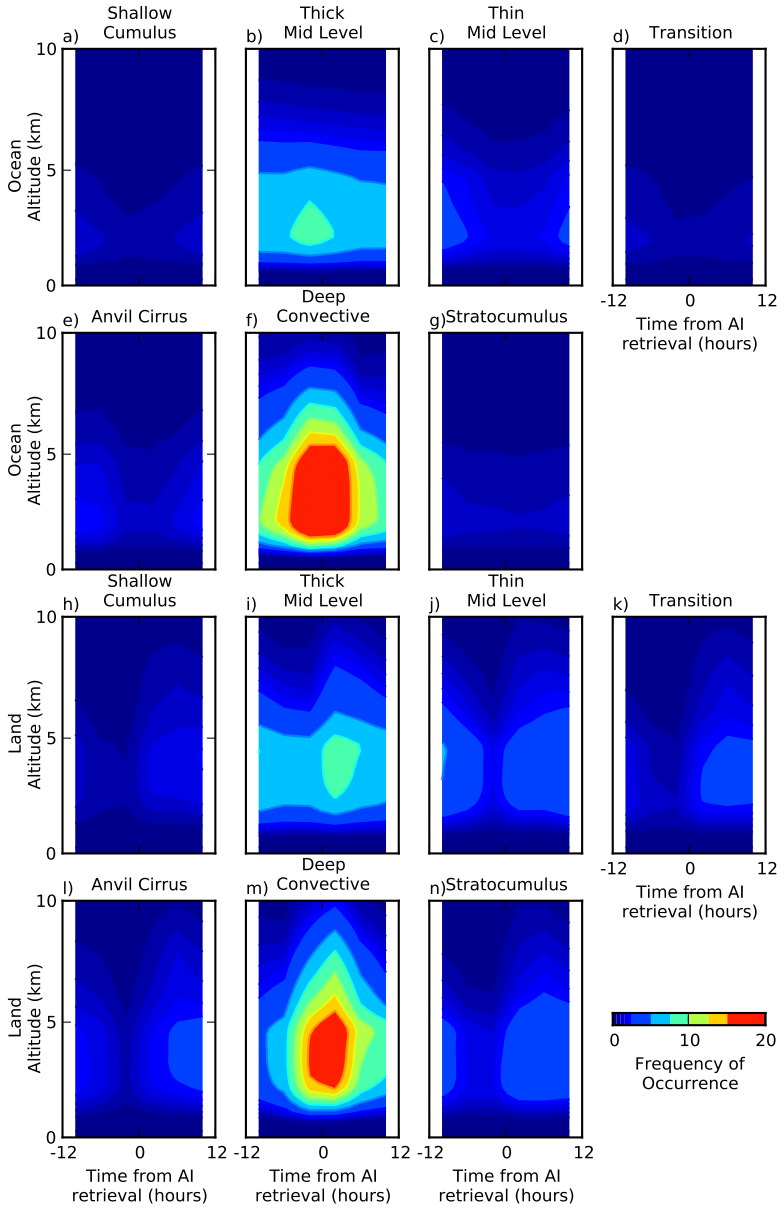

Figure A.1: The frequency of occurrence of reflectivities above 20 dbZ from the TRMM PR for each regime at times relative to 1330 LST over the period 2003-2007. These are from the TRMM 2A25 PR radar reflectivity product over the study region 30°N-30°S

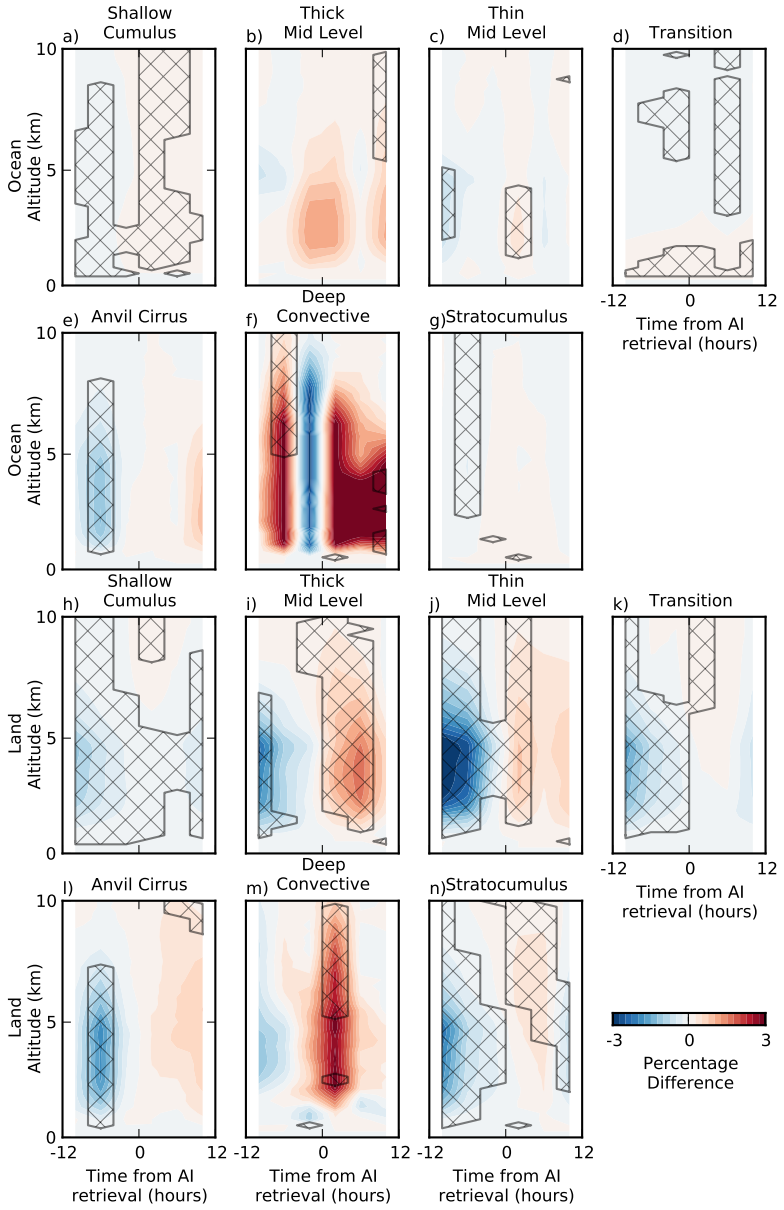

Figure A.2: The difference in the percentage of reflectivities above 20 dbZ from the TRMM PR between the high and low AI populations over the period 2003-2007. Red indicates an increase in >20 dbZ retrievals at high AI. The hatched areas show 95% significance in the change in frequency of occurrence.

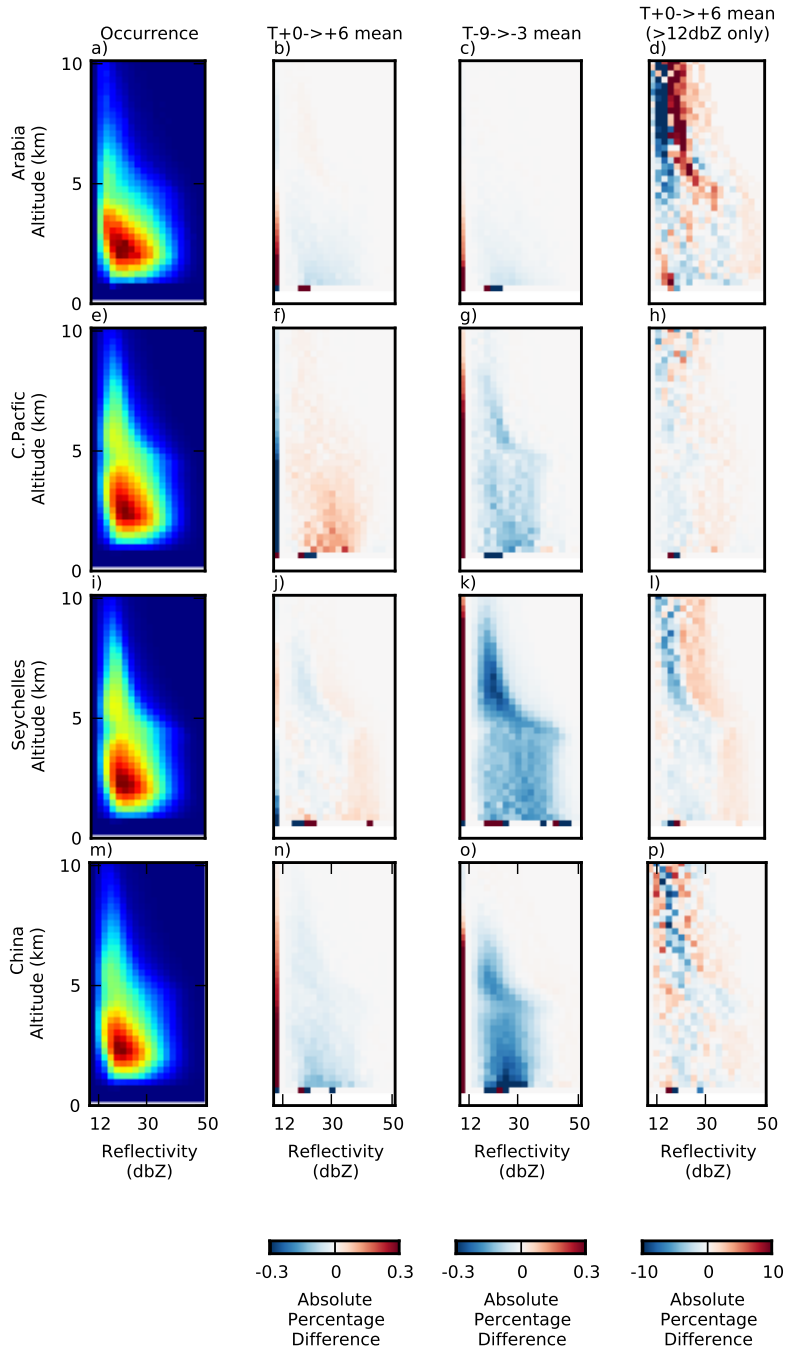

Figure A.3: (a,e,i,m) TRMM PR reflectivity-height histograms for the regions highlighted in figure 4. (b,f,j,n) shows the difference in the histograms for the low and high AI populations over the period T+0→+6. (c,g,k,o) show the difference for the time period T-9→-3. For these histograms, retrievals below 12 dbZ are included in the left-most column of the histogram. (d,h,l,p) show the difference in the histograms only including retrievals greater than 12 dbZ. For each of the plots, red indicates an increase with high AI and the difference histograms are normalised such that the changes sum to zero at each altitude. The right hand column is re-normalised, excluding pixels with a reflectivity below 12 dbZ.

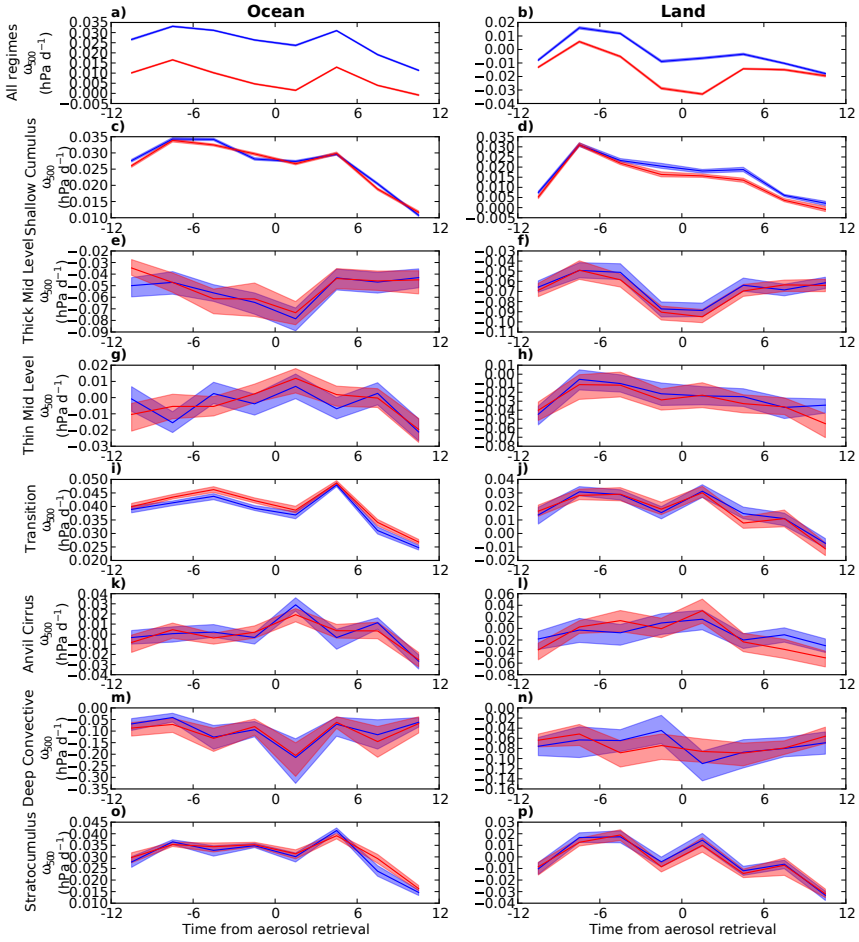

Figure B.1: The development of ECMWF ERA Interim 500 hPa pressure vertical velocity (ω_{500}) for the high (red) and low (blue) AI populations, for each of the regimes over the period 2003-2007. The error bars show the 95% confidence limits. As in Fig. 2, the difference in CF and ω_{500} between the high and low AI populations is removed at T+0.

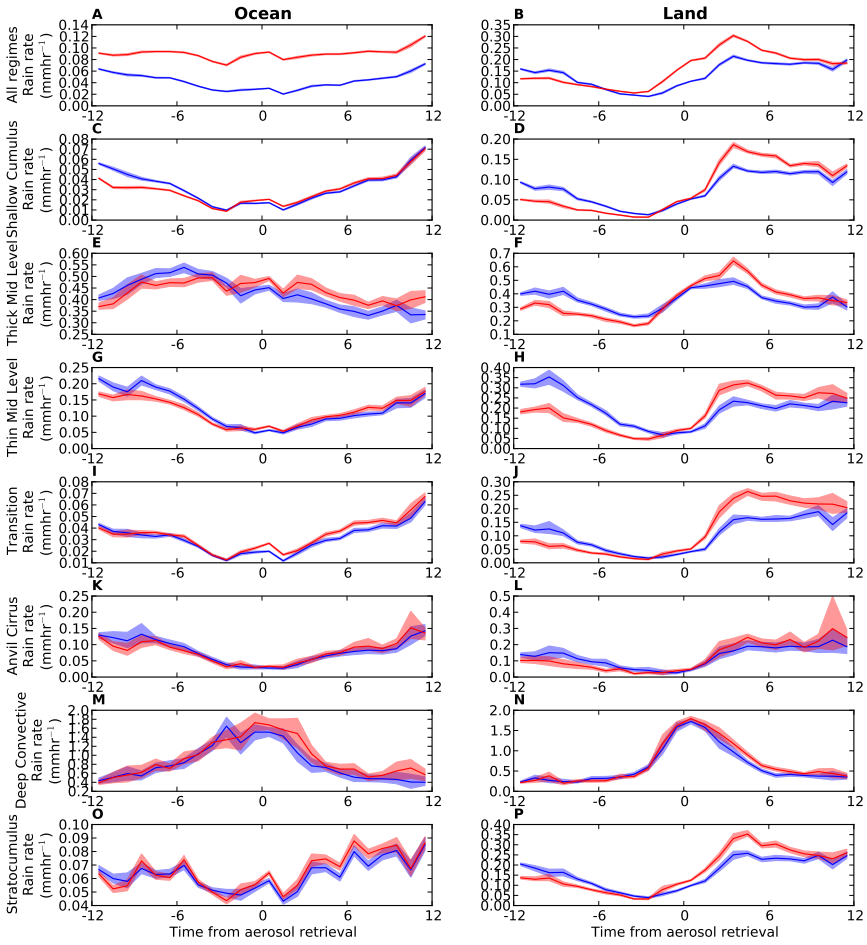

Figure C.1: As Fig. 2 but using the 'HQ' product, which is restricted to the microwave precipitation retrievals.

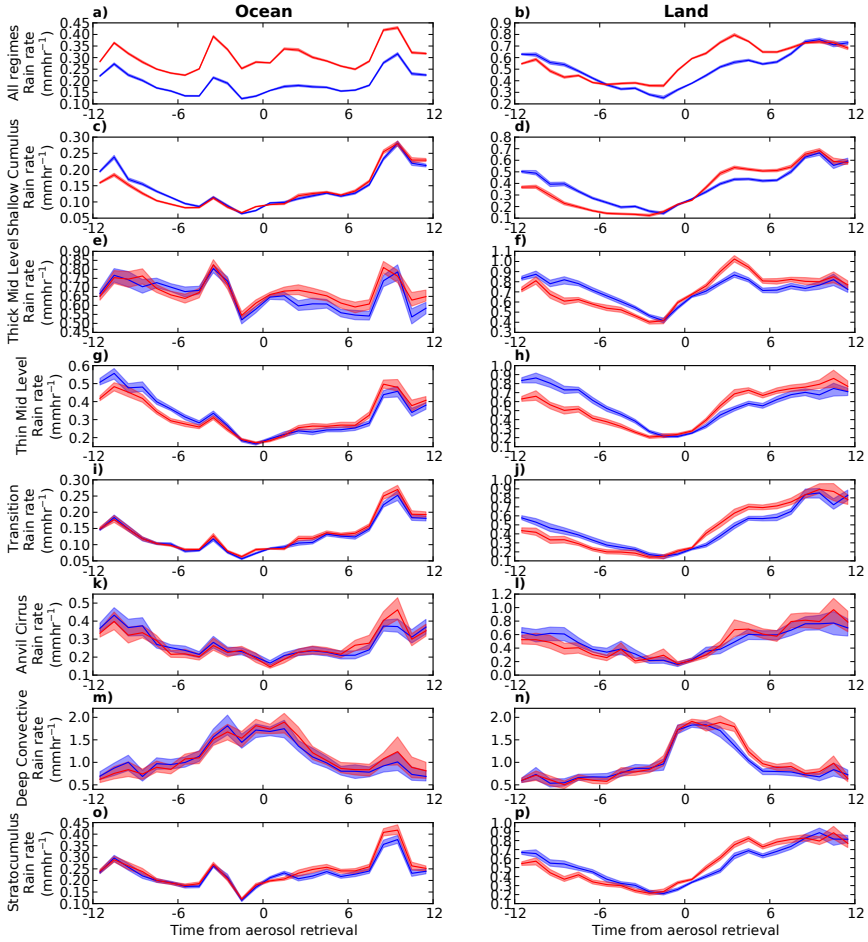

Figure C.2: As Fig. 2 but restricting the precipitation retrievals used to only those where precipitation is detected by the 3B42 precipitation product.

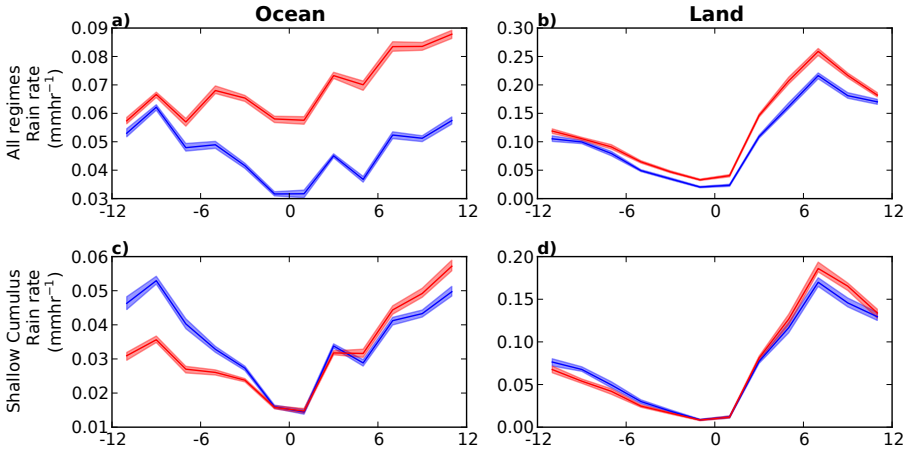

Figure C.3: As Figure 2 for the shallow cumulus regime and the regimes combined, but using the GlobAerosol AATSR AOD product over the years 2003-2007.

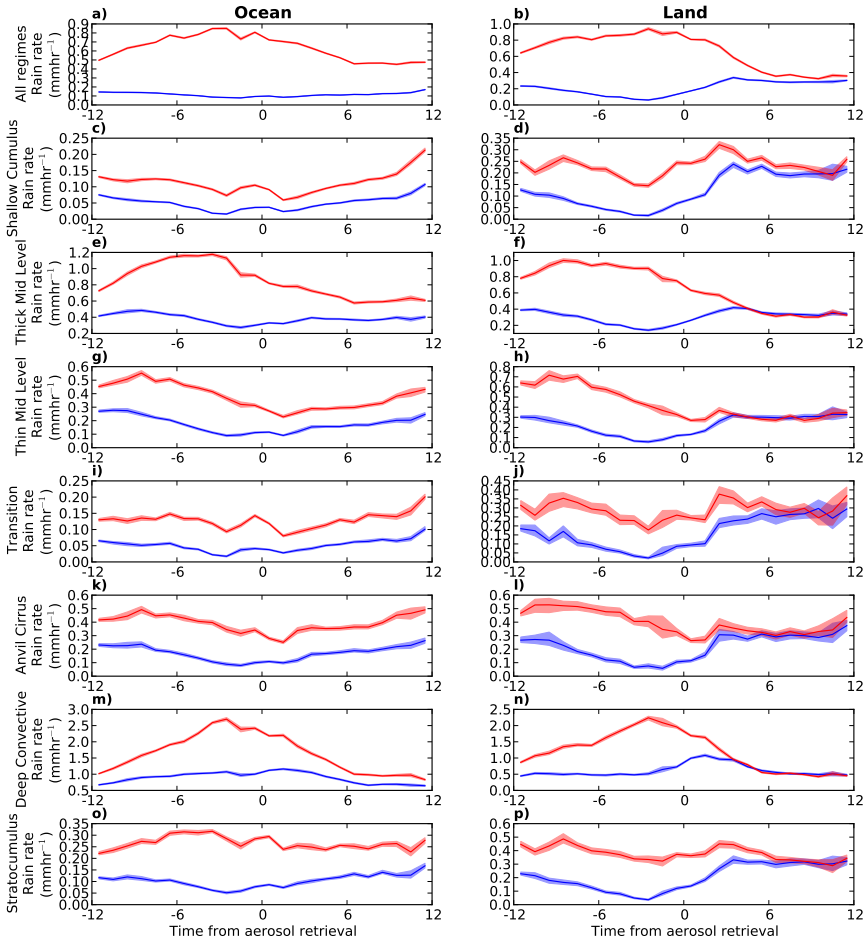

Figure C.4: As Figure 2 but using the precipitation rate at T-3 to define the high and low populations. The red line shows the precipitation rate of the highest quartile of precipitation rates at T-3 and blue the lowest quartile. The CF and meteorological property distributions are the same at T+0 for the high and low populations.

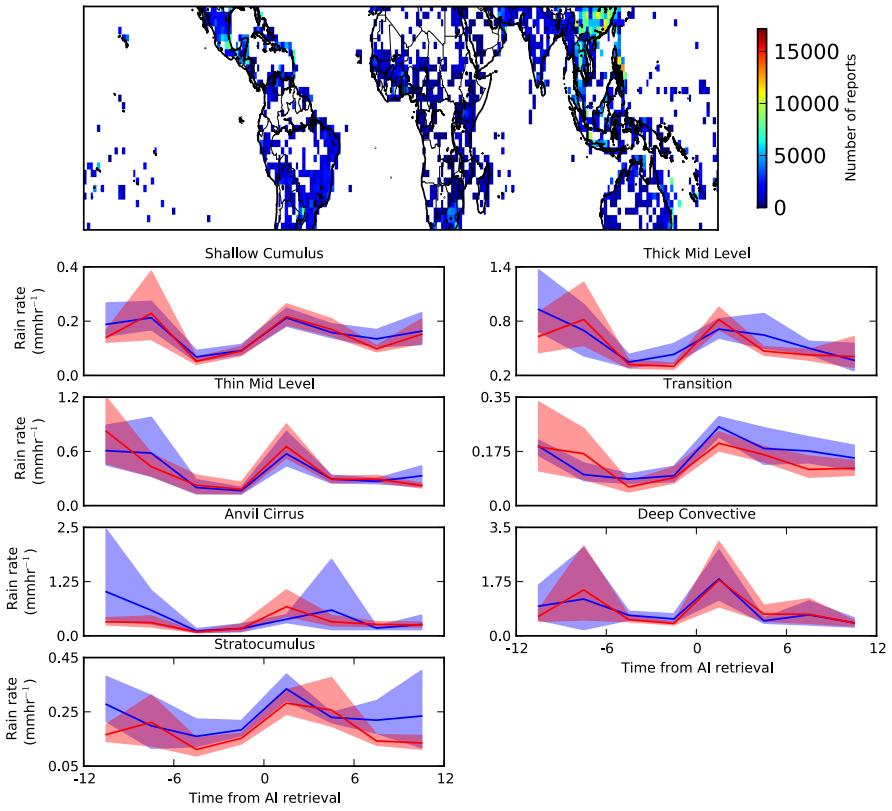

Figure D.1: a) The number of surface station precipitation reports over the period 2003-2011 from the UK Met. Office MIDAS database. For comparison, the 3B42 product would generate 12,000 reports per year for each of the 2° by 2° location shown here. b-h) Precipitation rates for each of the regimes at times before and after the Aqua MODIS AI retrieval (1330 LST). Red is the precipitation rate from the high AI population.